The effects of filling characteristics on the longitudinal forces developed in the braking train

Camil Ion Crăciun[1,*], and *Cătălin* Cruceanu[1]

[1]POLITEHNICA University of Bucharest-Romania, Department of Railway Vehicles, Bucharest, Romania

Abstract. Determination of longitudinal dynamic forces, size assessment as well as their distribution in the train body is, and will be a subject of global research. As observed from the beginning of the evolution of the railway vehicle and the train itself, the main reason for the occurrence of longitudinal dynamic forces is represented by the differences in inertial forces between the consecutive train vehicles. These inertial forces are influenced by the braking forces developed on each vehicle. The brake with which a railway vehicle is equipped is the pneumatic brake with compressed air. It evacuates the air from the train's general pipeline, increasing the pressure in the brake cylinders of each vehicle. The brake command and cylinder filling is more delayed on long trains compared to short ones. Thus, the brake can operate in two ways, the fast-action brake and the slow-action brake. In this paper, we aim to highlight the influence of the brake type by the brake cylinder filling characteristic of the dynamic longitudinal reactions. It will be analysed on a simplified train model the magnitude and distribution of longitudinal dynamic forces obtained using both braking systems.

1 Introduction

Rail vehicle braking is a complex and important process because it is directly involved in the safety of rail traffic. The complexity of the process is due to the multitude of mechanical, thermal or pneumatic phenomena that occur during braking. The phenomena appear and develop with varying intensities, all of which need to be inter-conditioned for one purpose, to ensure an efficient, correct and safe braking.

Nowadays, for railway transport, clear trends consist in a significant increase in traffic speeds, thus greatly reducing the time for passengers and goods transport, rail transport being in a fierce competition with air transport. Increasing traffic speeds is not just a matter of the design of the traction systems but also of how we can stop, on time and safely, these vehicles, so a significant problem is represented by the braking system used. Both during traction and braking a very important role is played by the wheel-rail adhesion, adhesion which, for very small values, can lead to skidding of the running gears (situations encountered in traction), but also to the locks of the wheels with adverse effects (situations encountered during braking).

* Corresponding author: craciun_camil@yahoo.com

Whether we are talking about classical trains or high-speed trains, it is necessary to use more complex braking systems and equipment in order to be able to stop or reduce their speed. From this point of view, at least two brake systems will be used, such as:

- adhesion brakes: the development and occurrence of the braking force is related to the adhesion between the wheel and rail. We can mention: the block brake used for speeds up to 160km/h, the disc brake used at speeds over 160km/h. These pneumatic braking systems cannot miss on high-speed railway vehicles because, regardless of the travelled space, they can stop at a fixed point, keep the trains on slopes, and they are automatic brakes (get into action in case of train break or alarm signal without the mechanic`s action on the system);
- dynamic brakes (brakes that do not use wheel-rail adhesion): speed reduction is not achieved by direct wheel-rail friction and does not develop braking force in stationary. These are used as additional brakes because they brake very well up to a certain critical speed where an adhesion-based braking system must necessarily take action.

Finally, we can say that the equipment of vehicles with braking systems has the main purpose of stopping at a fixed point and / or reducing speeds where there are restrictions for reasons of traffic safety.

Through this paper we want to bring into discussion and show the differences that may arise, from the point of view of the use of the brake type, between the longitudinal dynamic forces (LDF) developed in the body of brake trains that use slow and fast action brake.

1.1 Brake on railway vehicles

1.1.1 Pneumatic brake

Regardless of the railway vehicle, it should be noted that the U.I.C. no. 540 sheet [1] states that there must be a basic brake on the railway vehicle, namely the indirect compressed air brake, which, by its way of operation, is an automatic type brake. This brake system, although relatively simple from a constructive point of view, can stop the train safely, especially in the unfortunate situation where, for various reasons, a break may occur. The system is composed of the following elements shown in Figure 1, and it is the subject of many works including [2-3].

An important role in this braking system is played by the brake distributor - the assembly which controls the increase or decrease of pressure in the brake cylinder, but also the auxiliary tank which constitutes the compressed air reserve of the brake installation on the vehicle. The air distributor makes pneumatic connections between the general pipe and the auxiliary tank, the auxiliary tank and the brake cylinder, respectively between the brake cylinder and the atmosphere.

The indirect air brake operates on a simple principle: for the train brake loosening, pressurized air must be introduced into the system up to a pressure of 5 bars and for braking it is necessary to remove air from the installation sometimes, if the situation requires, an emergency brake up to 0 bars (thus the pressure in the pipe is equal to the atmospheric pressure).

In terms of operation, this braking system can be used in two ways [3]:

- as fast-acting brake (type P brake): usually used for short-trains, especially for passengers, or for short-freight trains running at speeds above 80 km/h. It is characterized by the fact that the filling time of the brake cylinder is 3 ... 5 s and the draining time of 15 ... 20 s;
- slow-action brake (type M brake): used for long-trains, generally for freight trains that have high tonnage and run at relatively low speeds. It is characterized by the fact that the filling time of the brake cylinder is 18 ... 30 s and the draining time is 45 ... 60 s.

In both situations, the pressure change in the train's general pipeline is detected by each distributor located along it, the time at which it senses and starts to operate depending on the speed of the brake wave propagation. In other words, the entry into action of each air distributor, and thus the development of braking force for each vehicle in the train body is done with a certain delay, thing highlighted and presented in numerous papers [4, 5, 6].

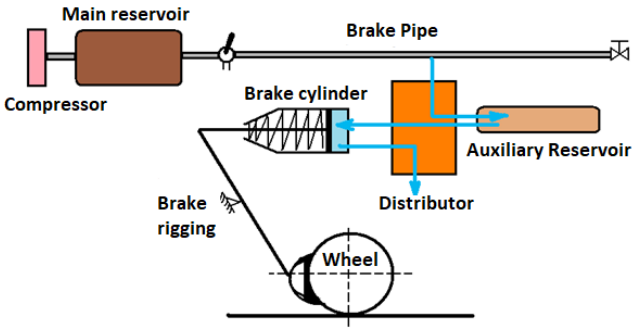

Fig. 1. Indirect compressed air brake.

From this point of view, between the consecutive vehicles of a train in braking mode, there are differences between the braking forces leading to the formation of LDF, with unfavourable effects on the passengers comfort, on the integrity of the transported goods and sometimes, even on the traffic safety. It can be said that, at some point in time, in the brake train body, the vehicles in the first half started to brake, while, the vehicles behind the train still have no braking force or have just begun to develop it. This aspect leads to collisions between the vehicles in the train body and thus LDF.

1.1.2 Braking force

Generally, the braking force acting on the rail vehicle depends on the characteristics of the braking system. According to Fiche U.I.C. 546, taking into consideration the circulation speed of the railway vehicles, there are two brake systems, namely:

- block brake system: used at vehicles running at speeds of less than 160 km/h;
- disc brake system: used at vehicles running at speeds above 160 km/h.

If the vehicle is equipped with block brake with symmetrical brake rigging, self-adjusting brake rigging fixed on the main brake bar, the braking force size can be calculated with the following formula [3]:

$$F_{fi}(t) = \left[\left(\frac{\pi d_{CF}^2}{4} \cdot p_{cf,i}(t) - F_R\right) \cdot i_c - R_{reg}\right] \cdot i_0 \cdot n_\Delta \cdot n_{cf} \cdot \mu_s(P_s, V_i) \cdot \eta_{tim} \quad (1)$$

where: d_{CF} - represents the diameter of the braking cylinder, $p_{CF,i}$ (t) – the value of the pressure at the time t; F_R – resistance force introduced by the back spring of the brake cylinder, i_c – central brake rigging ratio, i_0 – the axle brake rigging lever ratio, n_Δ - the number of triangular axis driven by the same brake cylinder, n_{CF} – the number of the active brake cylinders found on the vehicle, μ_s – the friction coefficient between shoe and wheel and η_{tim} – brake rigging efficiency.

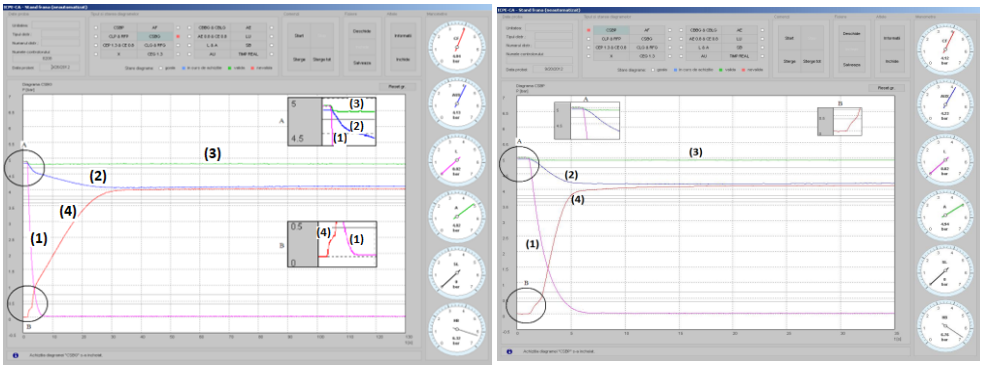

Fig. 2. Evolution of pressure in the brake cylinder a) slow-action brake, b) fast-action brake.
(1) - pressure in the general pipeline, (2) – pressure in the auxiliary reservoir, (3) – pressure in the control room, (4) – pressure in the brake cylinder.

If the vehicle is equipped with disc brakes, individual brake rigging, with brake cylinders having automatic brake rigging regulator incorporated in the piston rod, the size of the braking force can be determined [3]:

$$F_{fi}(t) = \left[\frac{\pi d_{CF}^2}{4} \cdot p_{cf,i}(t) - \left(F_R + R_{reg}\right)\right] \cdot i_t \cdot n_{cf} \cdot \mu_g \cdot \eta_{tim} \cdot \frac{2 \cdot r_m}{D_0} \quad (2)$$

where: d_{CF}, $p_{CF,i}$ (t), F_R, η_{tim} have the same meanings previously explained, i_t – the overall ratio of brake rigging amplification, n_{CF} – the number of active brake cylinders that equip the vehicle, r_m – the average friction radius between the brake lining and the disc, D_0 – the diameter of the wheel in the plane of the nominal running circle, μ_g – the friction coefficient between the brake lining and disc.

To be introduced into the simulation program, the two types of pressure shown in Figure 2 were experimentally determined on the specially designed stand of the Rolling Stock Department.

Based on these pressures and making sure that during braking the axles do not block, so to use at maximum the available adhesion force, formulas 1 and 2 can easily be transformed into [3]:

$$\boldsymbol{F_{f,i}(t) = \mu_a \cdot m_i \cdot g \cdot \frac{p_{cf,i}(t)}{p_{cf\,max}}} \quad (3)$$

where μa represents the wheel-track adhesion coefficient, and mi the mass of each vehicle in the train boy, pcfi(t)- evolution in time of the pressure in the brake cylinder, experimentally determined on the stand of the braking laboratory from Railway Vehicles Department, and pcfmax is the maximum stabilized pressure.

2 Longitudinal dynamic forces

In order to determine the magnitude of the longitudinal dynamic forces developed in the body of the trains in the braking regime, it is necessary to specify that they occur at the level of the buffer and draw-gear devices that maintain at a certain distance each vehicle in the train body.

Thus, the assessment of these forces depends to a large extent on the type and characteristics of these devices, but also on the mechanical model adopted for the railway vehicle. The following is a brief description of the mechanical model, the motion equations and the mathematical model used to determine the evolution of longitudinal dynamic forces over time.

2.1 Train model

The model chosen for the braked train is a simple model, very similar to those presented in the literature, consisting of n rigid bodies, representing the vehicles that are part of the train composition, connected by means of elastic and damping elements with which the buffer and draw-gear devices were modelled.

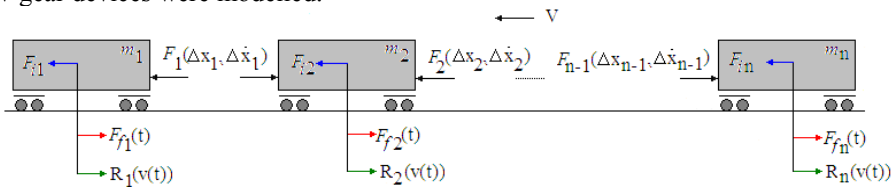

Fig. 3. Train model [8].

On each vehicle of mass m_i that enters in the train formation and moves with the speed V the following forces act: inertia forces F_{in}, braking forces $F_{fi}(t)$, resistances to motion $R_i(v(t))$ and the forces from buffer and draw-gear devices $F_{i-1}(\Delta x_{i-1}, \Delta x_{i-1})$, for $i = 1 \div n$, where with $\Delta x_i = x_i - x_{i+1}$ was noted the relative displacement from buffer and draw-gear devices (see Fig. 3). By applying the laws of mechanics we obtain n-1 nonlinear equations, each describing the movement between two consecutive vehicles. Generalizing, we can write the equation of movement between two vehicles i and i+1, thus:

$$y_i = \frac{F_i(y_i, y_i) - F_{i+1}(y_{i+1}, y_{i+1}) + F_{f,i+1}(t) + R_{i+1}(v(t))}{m_{i+1}} + \frac{F_i(y_i, y_i) - F_{i-1}(y_{i-1}, y_{i-1}) + F_{f,i}(t) + R_i(v(t))}{m_i} \quad (4)$$

The nonlinear equations are solved by numerical integration, thus determining the system state variables, the displacement and the relative speed between the vehicles, and then calculating the longitudinal forces developed in the buffer and draw-gear devices.

2.2 The model for buffer and drow-gear devices

In order to determine the static and dynamic characteristics of the collision devices, the experimental determinations on buffers with Ringfeder-type metallic rings, figure 3 present the characteristic diagram of the buffer which equips the freight vehicles built in Romania.

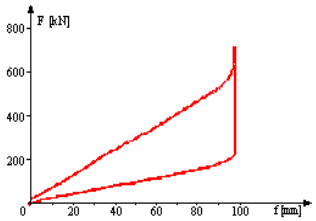

Fig. 3. The characteristic of the Ringfeder-type buffer used on freight trains.

Thus, the calculation of forces at the level of buffer and draw-gear devices is done by the relation [8]:

$$F_i(y_i, y_i) = \frac{(1 - sgn\ y_i)\left(k_e y_i + k_f |y_i| tanh(u y_i)\right) + (1 + sgn\ y_i)\left(k_{ec} y_i + k_{fc} |y_i| tanh(u y_i)\right)}{2} \quad (5)$$

where k_{ec} and k_{fc} represent specific constants for elastic and friction forces that develop in the traction device, k_e and k_f - specific constants for elastic and friction forces that develop in the collision device, and u represents a scaling factor.

3 Numerical applications

In this section there are shown the results of the numerical simulations concerning the evolution of LDF, as well as the distribution of maximum forces of compression and stretching that develop in the buffer and draw-gear devices of a train subject to a rapid braking action at a maximum speed of 120 km/h, on a path located in alignment and landing.

It was assumed that the train composition includes the locomotive mass m_l and the wagons with each value m_v. The numerical simulation parameters are shown in Table 1.

The results of the simulations are shown in Figures 4 … 6 for the G-type brake case, and for the P-type brake are shown in Figures 7 ... 9. The operation of the G-type brake is observed in the way the LDF evolve in time (Fig. 4), where the peaks are characteristic of the compression of the tampons when there are significant differences between the braking forces of the consecutive vehicles. There follows a relative retention as the braking forces equalize, after which, the rebound-specific stretching forces appear in the literature. Further more, it can be seen that, although at much lower values, a damped oscillatory motion specifies the longitudinal oscillatory movement during train braking.

In terms of compressive forces, they reach maximum values on vehicles near the middle of the train (Fig. 5), while the stretching forces show an almost symmetrical distribution relative to the number of couplings (Fig. 6). The maximum compression force is 52 kN on coupling 11 (vehicles 11-12), while stretching force barely reaches 8 kN on coupling 8 and 9 (vehicles 8-10).

Passing the changeover to the P position leads to a modification of the brake cylinder filling time and hence significant changes in the evolution of the LDF in the train body (Fig. 7). It is noticeable how the train compression is followed by its rebound and the appearance of a strong oscillatory movement this time with the major demands of the crash and coupling traction devices. Observing Figure 8, we find that the maximum compression forces retain somehow the altitude, but the values are three times larger, reaching 160 kN compared to the above, on the couplings 11 and 12.

Table 1. Parameters of the numerical simulation.

The mass of the locomotive	m_l = 120 t	
The mass of a wagon	m_v = 60 t	
Specific constants for collision devices	$k_e = 4{,}1 \cdot 10^6$ N/m	$k_f = 2{,}1 \cdot 10^6$ N/m
Specific constants for traction and binding devices	$k_{ec} = 5{,}46 \cdot 10^6$ N/m	$k_{fc} = 2{,}43 \cdot 10^6$ N/m
Scaling factor	$u = 10^4$	
Maximum pressure in braking cylinder	$p_{cf\max} = 3.8 \pm 0{,}1$ bar	
Wheel-rail adhesion coefficient	$\mu_a = 0.1$	

The situation is similar in the case of stretching forces. The maximum forces being present in the first half of the train, the values being very high compared to the previous case reaching values of about 93 kN on the couplings 8 and 9.

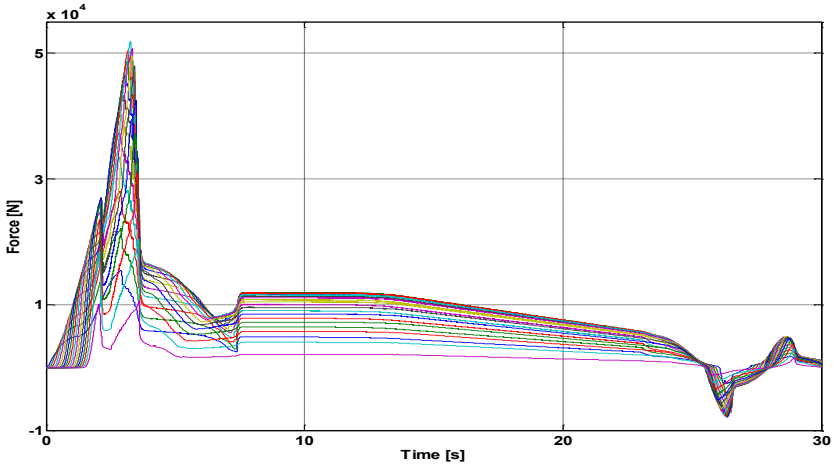

Fig. 4. LDF – slow-action brake.

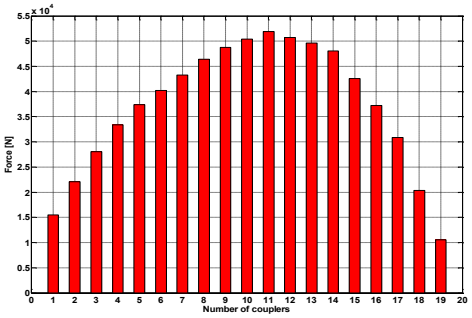

Fig. 5. Distribution of compression forces – slow-action brake.

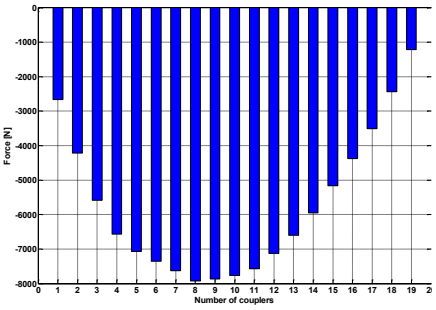

Fig. 6. Distribution of tensile forces – slow-action brake.

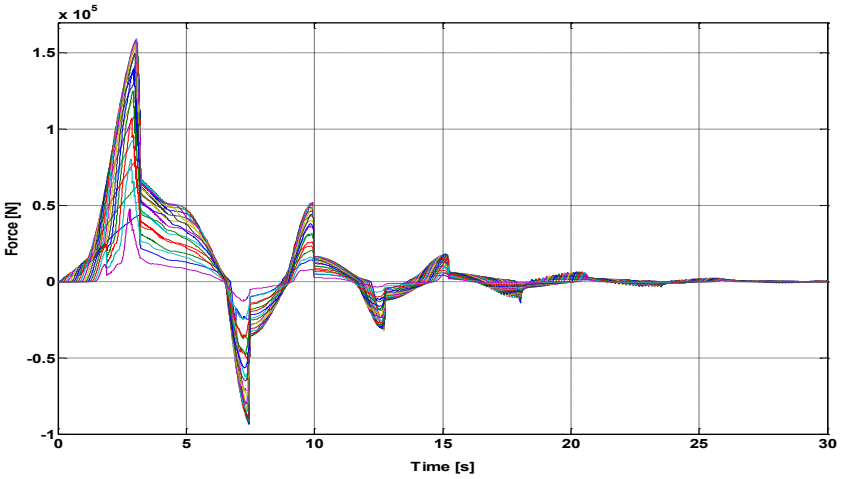

Fig. 7. LDF – fast-action brake.

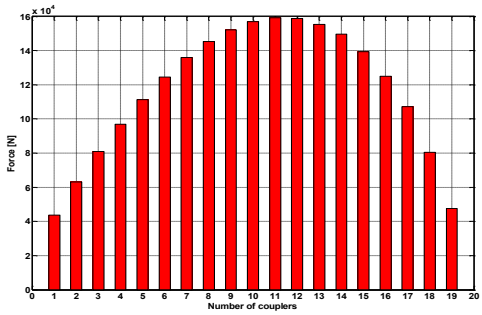

Fig. 8. Distribution of compression forces – fast-action brake.

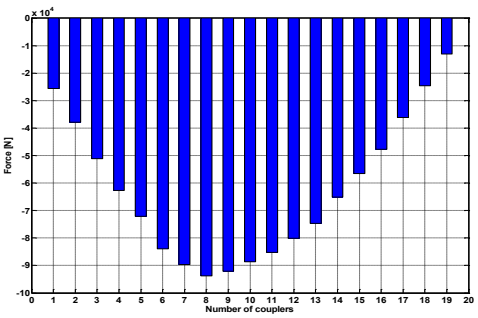

Fig. 9. Distribution of tensile forces – fast-action brake.

It can be concluded that, for the characteristics of a freight train, the use of a quick-action brake instead of a slow-action brake will require a great deal of crash and bindings, although the forces obtained in this situation fit smoothly within the range indicated by the functioning of these devices.

Conclusion

Analysing the evolution and distribution of the LDF for a train under the conditions in which the P-type brake or the G-brake is used, the following conclusions can be drawn:

- the use of the G-type brake leads to a decrease in the forces required by the traction and binding crashes due to a long evolution of the LDF,
- switching the P-type brake has the effect of tripling the compression forces of the buffers and the increase of about 10 times the tensile forces on the traction hooks,
- the longitudinal oscillatory movement of the train is significantly reduced for the G type brake compared to the P type, where the phenomenon is much stronger and the stretch compression cycles alternate much more often.

As a result of the study, we can recommend avoiding as far as possible P-type freight traffic situations because the collision and coupling traction devices are strongly solicited compared with the use of the type G brake.

This work has been funded by University Politehnica of Bucharest, ARUT-GNac2018, 8/2019, ID 94/2018.

References

1. UIC leaflet 540: *Brakes - Air Brakes for freight trains and passenger trains*, 5th edition (2006)
2. L. Pugi, D. Fioravanti & L. Rindi, *12th IFToMM World Congress* (2007)
3. C. Cruceanu, *Train Braking* (Xavier Perpinya InTech), 29-74 (2012)
4. L. Pugi, M. Malavezzi, S. Papini, G. Vellori, J. of Modern Trans. **21**, 247-257 (2013)
5. C. Cole *Longitudinal train dynamics* (Taylor & Francis Grup), (2006)
6. L. Pugi, M. Malavezzi, B. Allotta, L. Banchi, P. Presciani, Proc. IMechE **218,** F: J. Rail and Rapid Transit (2004)
7. C. Cruceanu, C.I. Crăciun, I.C. Cruceanu, **87**, 3-33 Springer Int (2017)
8. C. Crăciun, M. Dumitriu, *Appl. Mech. Mater.*, **809-810** 6 (2015)